ChemPlusChem

A Multidisciplinary Journal Centering on Chemistry

Chemistry Europe

European Chemical Societies Publishing

Accepted Article

Title: Ethylene Tetramerisation: A Structure-Selectivity Correlation

Authors: Boitumelo Francinah Makume, Cedric W. Holzapfel, Munaka C. Maumela, J. Alexander Willemse, and Jan A. van den Berg

To be cited as: *ChemPlusChem* 10.1002/cplu.202000553

Link to VoR: https://doi.org/10.1002/cplu.202000553

WILEY-VCH

Ethylene Tetramerisation: A Structure-Selectivity Correlation

Boitumelo F. Makume,*[a,b] Cedric W. Holzapfel,[a] Munaka C. Maumela,[a,b] J. Alexander Willemse[b] and Jan A. van den Berg[b]

[a] Dr B.F. Makume, Prof. C.W. Holzapfel, Prof. M.C. Maumela
Department of Chemical Sciences
University of Johannesburg
Kingsway Campus, Aucklandpark, 2006, South Africa
E-mail: boitumelo.makume1@sasol.com

[b] Dr B.F. Makume, Prof. M.C. Maumela, Dr J.A. Willemse, Dr. J.A. van den Berg
Group Technology
Sasol South Africa
1 Klasie Havenga road, Sasolburg, 1947, South Africa

Supporting information for this article is given via a link at the end of the document.

Abstract: The effect of ethylene tetramerisation ligand structures on 1-octene selectivity is well studied. However, by-product formation is less understood. In this work, a range of PNP ligand structures are correlated with the full product selectivity as well as with catalyst activity. As steric bulk on the N-substituent increases, the product selectivity shifts from >10 % C6 cyclics and C16+ by-products respectively, to ca. 70 % 1-octene and finally to 1-hexene. Similar changes in selectivity were observed for *ortho*-Ph-substituted PNP ligands. The C10-14 selectivity was hardly affected by ligand structural changes. The ligand effect on the systematic shift in selectivity can be explained mechanistically. Furthermore, an increase in ligand steric bulk was found to improve catalyst activity and reduce polymer formation by an order of magnitude. It is proposed that steric bulk promotes formation of cationic catalytic species which are responsible for selective ethylene oligomerisation.

Introduction

The first selective ethylene tetramerisation catalyst was described by Sasol in 2004.[1-2] Both selective trimerisation and tetramerisation are thought to involve metallacyclic intermediates (Scheme 1).[1-2]

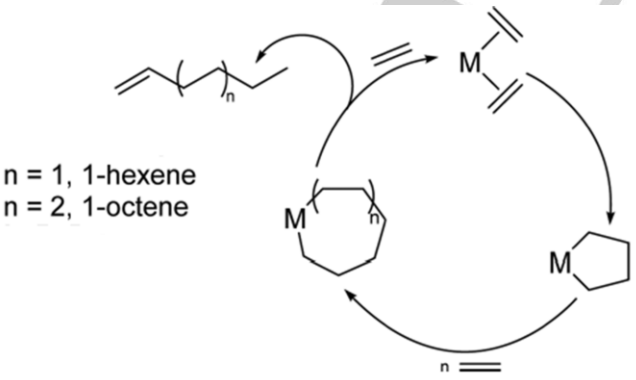

Scheme 1. Metallacyclic mechanism for selective ethylene trimerisation and tetramerisation.

The Sasol catalyst consists of a chromium source, methylaluminoxane (MAO) as the co-catalyst/activator, and a diphosphinoamine (PNP) ligand. A representative system is shown in Scheme 2. Upon its discovery, this catalytic system was not only selective towards 1-octene but also highly active (0.59 x10^6 g/gCr/h).

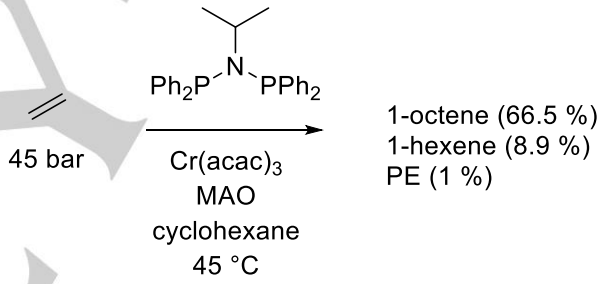

Scheme 2. A representation of the Sasol tetramerisation process.

Due to the high demand and value of 1-octene as a co-monomer in the production of LLDPE (linear low density polyethylene), the commercial and industrial potential of the Sasol catalyst was immediately realised. Consequently, extensive experimental and theoretical studies were undertaken to understand the catalytic process [3-12] and to improve product selectivity and catalyst activity.[13-14]

One of the initial strategies to optimise selectivity with the PNP ligands included modification of the N-substituent.[15] These studies showed an initial increase in the selectivity to 1-octene with increasing steric bulk on the N-substituent, up to a maximum. A further increase in steric bulk resulted in a decrease in 1-octene selectivity. In an attempt to quantify the bulk around the N-atom in PNP ligands an “effective Tolman-based N-substituent steric parameter” (θN-sub, Figure 1) derived from crystallographic and computational data was defined.[16]

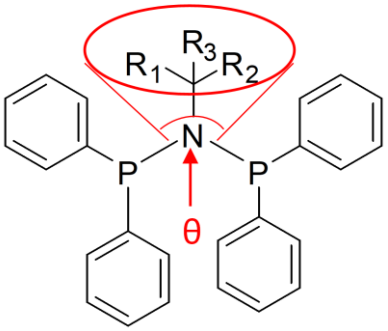

Figure 1. Effective Tolman-based θN-sub calculation.[16]

It was further shown that a clear relationship exists between this steric parameter and the 1-hexene and 1-octene selectivities attained from catalysis with PNP-based Cr complexes.[16] The results suggested that the N-alkyl group transmits its steric bulk to the gross steric properties of the ligand which impact directly on the catalytic pocket (i.e. the area where the metallacycle grows) of the Cr-ligand complex.

A number of different approaches to quantify ligand steric bulk have been described in the literature. Recently, a web tool (SambVca 2) has been used to analyse catalytic pockets with the aid of topographic steric maps.[17] Previously, Cavallo and his group developed a method for determining "percent buried volume, % Vbur", which is defined as the fraction of the total volume of the coordination sphere of the metal occupied by a specific ligand.[18-19] Maley et al.[20] recently utilized % VBur, along with other catalyst features obtained from experimentally verified DFT-transition-state models, to design a new generation of Cr phosphine imine catalysts with high 1-octene selectivity. Another measure of ligand steric bulk is its G-parameter, G-parameters illustrate the extent to which the ligand shields the central metal and the extent of steric saturation in the coordination sphere of the metal (Figure 2).[21] The G-parameter can therefore indicate the possibility of additional ligand incorporation in the metal coordination sphere.[22]

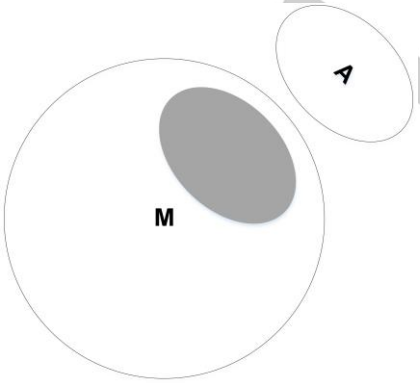

Figure 2. Illustration of the G-parameter: A percentage of the area occupied by the shadow casted by ligand **A** when the central metal **M** is replaced by a light source.[21]

Information on Vbur and G-parameters of Cr-ligand complexes as pre-catalysts for ethylene oligomerisation can be obtained from crystallographic data.[23-27] All the available data confirm the tendency to firstly increase and then reduce 1-octene selectivity with increasing steric bulk. However, these studies have provided little information with regards to by-product formation (i.e. C6-cyclic products, C10-C14 secondary incorporation products, C16+ products and polymer), which is of cardinal importance from a commercial point of view. This work aims to correlate ligand structural properties with the full product selectivity (i.e. 1-octene, 1-hexene and by-products) as well as catalyst activity.

Results and Discussion

The optimised geometries of some of the putative metallacyclic intermediates were previously determined by molecular modelling using DFT intermediates in the DMol^3 code.[28] The optimised PNP ligated chromacycloheptanes yielded a distorted geometry in which one of the metallacycle α-carbons occupies an axial position. The ligand P donor atoms as well as the second metallacycle α-carbon occupied equatorial positions. A prominent agostic β-H (β-H to Cr distance is near 1.955 Å in all optimised geometries) occupied the remaining equatorial position. This left an axial position vacant for ethylene coordination, since Cr(III) complexes normally accommodate six ligands in their coordination spheres. A schematic representation of an ethylene coordinated generalised PNP-ligated chromacycloheptane is shown in Figure 3.

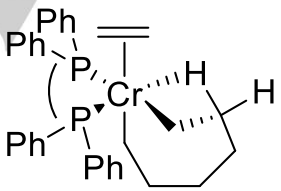

Figure 3. Putative structure of PNP-ligated and ethylene-coordinated chromacycloheptane

In light of the proposed optimimum geometry of the PNP-ligated chromacycloheptane, herein, the product selectivity of a wide range of PNP ligands that were previously prepared and tested by the Sasol research group is correlated to the ligand structural features. All the data was generated under standard conditions, in the same laboratory. This is particularly important to minimise catalyst performance variations due to differences in reagent purity or reaction conditions.

The effect of changes of the N-substituents (R) in $Ph_2PN(R)PPh_2$ ligands

PNP ligands with varying substituents on the N-atom were evaluated (Figure 4). Table 1 shows the effect of changes of the N-substituent (R) in $Ph_2PN(R)PPh_2$ on product selectivity and catalyst activity.

The results only indicate liquid product selectivity and do not include polyethylene (PE) by-product formation which represents less than 1.5 % and generally no more than 0.5 % of the total product. Ethylene uptake was controlled to a product:solvent ratio of 1.5 to 1.75.

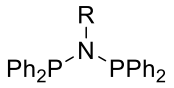

1a: R = CH_3

1b: R = nBu

2: R = $CH_2CH(CH_3)_2$

3: R = $CH(CH_3)_2$

4: R = 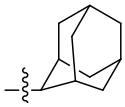

5: R = $CH(CH_3)CH(CH_3)_2$

6: R = $C(CH_3)_3$

7: R = 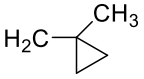

8: R = $CH_2C(CH_3)_3$

Figure 4. PNP ligands with varying N-substituents.

Table 1. Activity and product selectivity of $Ph_2PN(R)PPh_2$ ligands.[a]

Entry	Ligand	Activity [10^6 g/gCr/h]	Product selectivity [mass %]				
			1-C6	C6 cyclics	1-C8	C10-14	C16+
1	1a	0.8	5.2	10.1	53.3	14.3	11.2
2	1b	1.0	6.7	9.2	61.0	11.8	7.4
3	2	1.1	8.6	9.5	65.1	9.6	3.9
4	3	1.5	14.1	4.1	68.9	9.1	2.1
5	4	2.5	25.1	2.8	61.0	9.3	0.5
6	5	3.8	18.9	3.2	67.0	9.5	0.9
7	6	1.1	30.4	1.8	57.8	10.3	0.6
8	7	1.5	24.7	2.6	63.6	9.0	0.5
9	8	1.0	40.6	1.0	47.5	10.3	0.4

[a] Conditions: 100 mL Methylcyclohexane (MCH), 2.5 µmol $Cr(acac)_3$, 1.1 equiv. ligand, 960 equiv. Al, 45 bar, 60 °C, ethylene fed to reactor = 160g. 1-C8 = 1-octene, 1-C6 = 1-hexene.

The results showed that an increase in ligand steric bulk on the N-alkyl group firstly results in a shift from C16+ and then from C6-cyclic by-products mainly to 1-octene and 1-hexene. This suggests that the pathway involved in C6 cyclic and C16+ products is extremely sensitive to the steric bulk of the ligand. The results also suggest that there is an upper limit for 1-octene selectivity, beyond which any further increase in ligand steric bulk results in a decrease in 1-octene and further increase in 1-hexene selectivity. A similar trend was observed in previous work whereby different N-alkyl[15] and N-cycloalkyl[29] groups in PNP ligands were studied. In both cases, 1-octene selectivity increased up to a peak (N-iPr and N-cycloheptyl respectively) before declining, while 1-hexene selectivity continued to increase. C6 cyclics and C16+ decreased linearly with increasing steric bulk. At the similar product:solvent ratios, the C10-14 by-product formation does not change significantly with changes in ligand steric bulk. Thus indicating a relative independence of this product to ligand structural features.

Interestingly, DFT models of the PNP-ligated chromacycloheptane intermediates for ligands **1** to **8** revealed that the smallest Cr-P-Ph angle and the G-parameter correlated well with the changes in product selectivity (graphs included in supporting information): The reduction in by-products and increase in 1-octene and 1-hexene selectivity was generally associated with a smaller intrusion angle (i.e. larger P-phenyl intrusion into the catalytic pocket) and a larger G-parameter (i.e. larger steric bulk).

The systematic shift in selectivity with increasing steric bulk (i.e. from C6 cyclics and C16+ to 1-octene and then to 1-hexene) is supported by the recent DFT-based reaction mechanisms[30-31] (Scheme 3) which suggest that C6 cyclics and C16+ products share a common intermediate (**H**, which is most sterically demanding), while 1-hexene and 1-octene are each derived from different intermediates (**D** and **F** respectively). All three intermediates are interconnected and affected differently by ligand steric bulk.

As a consequence of the different steric effects on the competing pathways, it is reasonable to expect (as evident in the results of Table 1) that a selectivity of ca. 70 % may be optimal for 1-octene formation for ligands with a $Ph_2PN(R)PPh_2$ structural motif. To date, there has been no report of 1-octene selectivities more than 70 % with PNP ligands (particularly at ≤ 45 bar ethylene pressure).

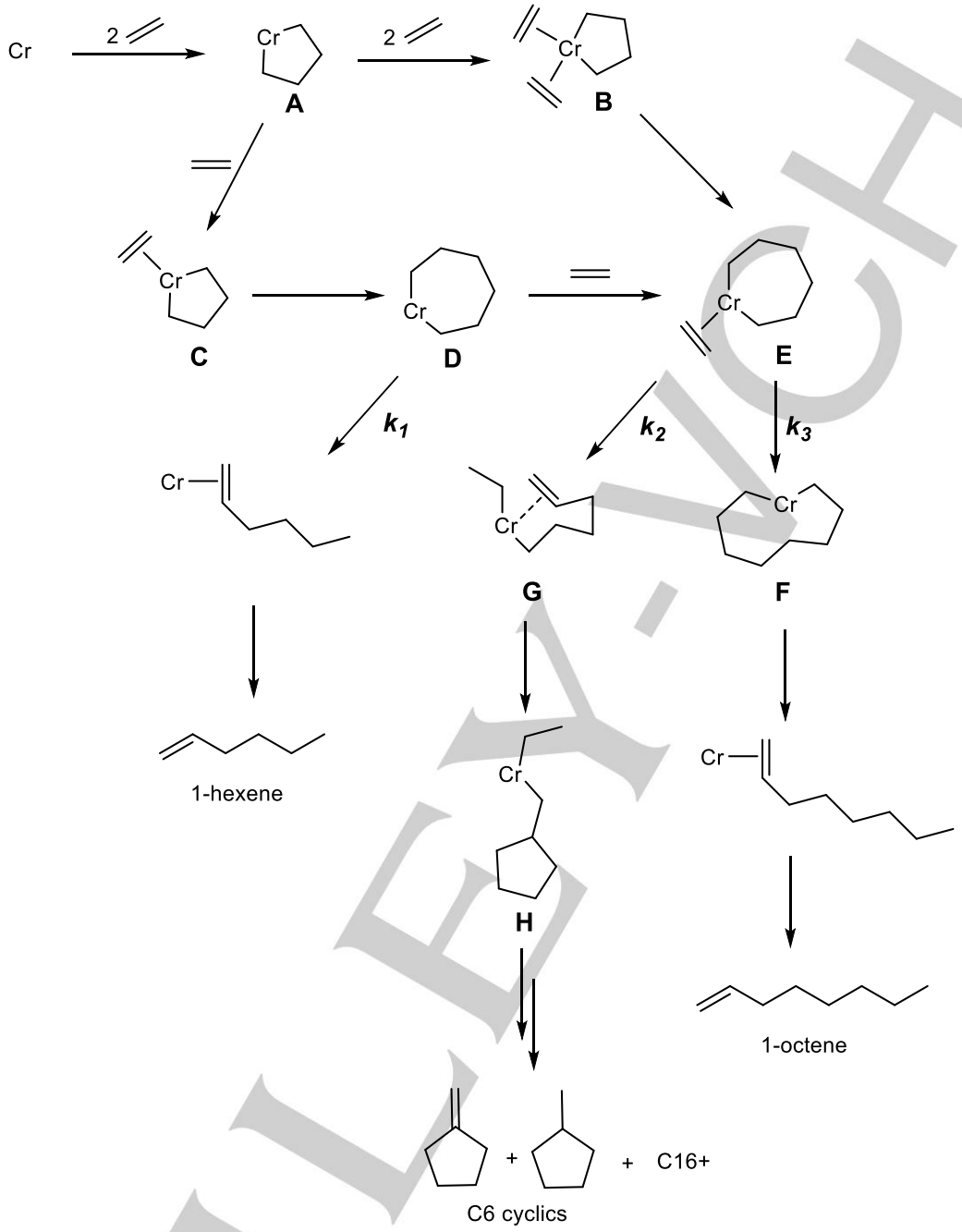

Scheme 3. DFT-based mechanistic model for selective ethylene oligomerisation.

The effect of substitution on the phenyl groups in $Ph_2PN(R)PPh_2$ ligands

The effect of substitution of the phenyl groups of $Ph_2PN(R)PPh_2$ ligands on 1-octene selectivity has also received considerable attention. A DFT-based study indicating how alkyl substituents at *ortho*-positions of PNP phenyl groups suppress the available pathway to 1-octene has also been reported.[32] The effect of *ortho*-alkyl substitution on product selectivity and catalyst activity is investigated further in this section. The ligand structures are shown in Figure 5. Table 2 summarises the catalytic data.

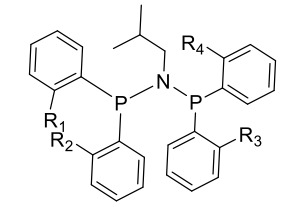

9: $R_1 = CH_3$, $R_2 = R_3 = R_4 = H$

10: $R_1 = R_2 = CH_3$, $R_3 = R_4 = H$

11: $R_1 = R_3 = CH_3$, $R_2 = R_4 = H$

12: $R_1 = R_2 = Et$, $R_3 = R_4 = H$

13: $R_1 = CH(CH_3)_2$, $R_2 = R_3 = R_4 = H$

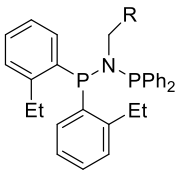

14: R = cyclohexyl

15: R = cyclopropyl

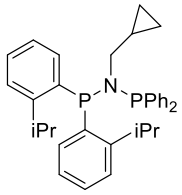

16

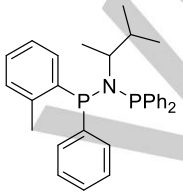

17

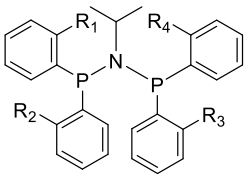

18: $R_1 = Et$, $R_2 = R_3 = R_4 = H$

19: $R_1 = R_2 = CH_3$, $R_3 = R_4 = H$

20: $R_1 = R_2 = Et$, $R_3 = R_4 = H$

21: $R_1 = R_3 = Et$, $R_2 = R_4 = H$

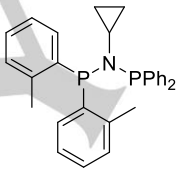

22

Figure 5. *Ortho*-substituted Ph_2PNPPh_2 ligands.

Table 2. Activity and product selectivity of o*rtho*-substituted Ph_2PNPPh_2 ligands.[a]

Entry	Ligand	Activity [10^6 g/gCr/h]	Product selectivity [mass %]				
			1-C6	C6 cyclics	1-C8	C10-14	C16+
1	2	1.1	8.6	9.5	65.1	9.6	3.9
2	9	1.2	17.3	12.3	60.4	7.4	1.7
3	10	5.0	27.5	3.4	61.4	6.9	0.5
4	11	3.2	34.7	5.6	52.7	6.0	0.3
5	12	4.7	31.8	3.7	57.5	5.9	0.5
6	13	2.8	32.1	7.9	52.1	6.4	0.6
7	14	3.7	33.5	3.3	56.3	5.8	0.6
8	15	3.7	30.3	3.7	58.0	6.7	0.5
9	16	3.1	25.7	4.6	57.5	7.1	4.2
10	17	4.3	42.6	4.4	43.6	6.5	0.3
11	3	1.5	14.1	4.1	68.9	9.1	2.1
12	18	3.0	28.4	5.8	56.8	7.4	0.7
13	19	4.5	38.7	1.4	49.4	8.8	0.6
14	20	4.3	27.2	3.0	58.4	8.4	1.2
15	21	3.3	62.3	3.0	26.8	5.3	0.1
16	22	3.3	26.9	4.1	60.5	7.0	0.6

[a] Conditions: 100 mL Methylcyclohexane (MCH), 2.5 µmol $Cr(acac)_3$, 1.1 equiv. ligand, 960 equiv. Al, 45 bar, 60 ˚C, ethylene fed to reactor = 160g. 1-C8 = 1-octene, 1-C6 = 1-hexene.

It can be seen from Table 2 that the introduction of *ortho*-alkyl substituents on the phenyl group(s) of the PNP ligands also shift product selectivity away from 1-octene, as well as from C6 cyclics and C16+ by-products. However, the effects are more dramatic than in the case of changes in the N-substituent, since *ortho*-substituents are more likely to directly impinge on the catalytic pocket.

It is of interest to note the vastly different product selectivities which result from the unsymmetrically di-substituted ligands **10** and **20** compared to the corresponding symmetrically di-substituted ligands **11** and **21** respectively (see Table 2). In these four cases, the unsymmetrically di-substituted ligands show considerably higher 1-octene selectivity.

To investigate this further, putative chromacycloheptane intermediate structures of ligands **10**, **11**, **20** and **21** were calculated. Interestingly, it was observed that in the case of the putative metallacyclic intermediates of ligands **10** and **20**, the two substituted phenyl groups are located on the side of the agostic βH (Figure 6). This is the least sterically crowded coordination position and thus allows optimal minimisation of opposing steric interactions. With ligands **11** and **21**, one of the substituted phenyl groups will inevitably interact with the bulkier α-carbon on an equatorial position of the metal (Figure 7).

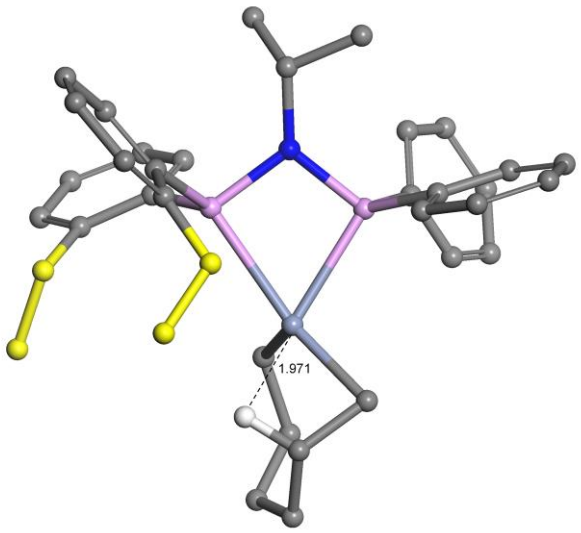

Figure 6. A DFT-generated structure of the putative intermediate corresponding to ligand **20** (all hydrogen atoms, except for the agostic βH, are omitted and *ortho*-ethyl groups are highlighted in yellow for clarity. βH-Cr distance is indicated in Å).

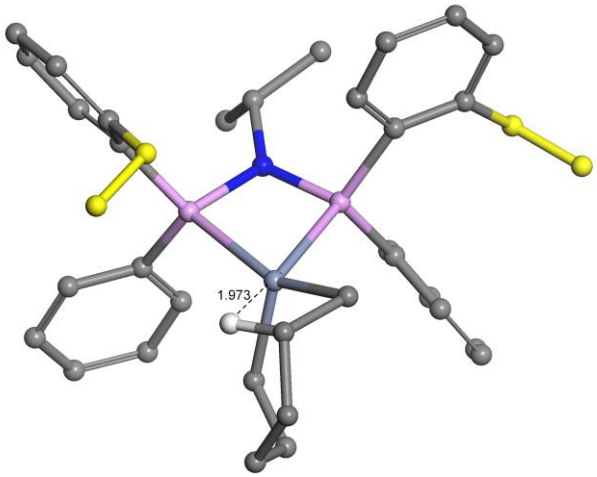

Figure 7. A DFT-generated structure of the putative intermediate corresponding to ligand **21** (all hydrogen atoms, except for the agostic βH, are omitted and *ortho*-ethyl groups are highlighted in yellow for clarity. βH-Cr distance is indicated in Å).

This tentative proposal that unfavourable steric interactions can be minimized in unsymmetrically di-substituted ligands is further supported by the marginal difference in 1-octene selectivity observed between the mono-substituted ligand **18** and the unsymmetrically di-substituted ligand **20**, as opposed to the much larger selectivity difference between ligand **18** and the symmetrically di-substituted ligand **21**. The same trend applies when ligands **9**, **10** and **11** are compared.

Correlating ligand structure with catalytic activity and polyethylene (PE) formation

The results in Table 2 also show an initial increase in catalyst activity with increasing ligand steric bulk, followed by a decrease in activity as the steric bulk is increased further. A similar trend was also evident when the steric bulk was increased on the N-substituent (Table 1). The initial rise in activity could possibly be due to steric acceleration of the reductive elimination steps.[33-35] Reductive elimination may be expected to result in a release of steric strain in the metallacycle intermediates. However, further increases in ligand steric bulk will restrict access of ethylene to the Cr coordination centre, thus reducing activity.

PE is a ubiquitous by-product of most selective ethylene oligomerisation reactions.[14] The formation of even small amounts of PE could result in significant reactor or downstream fouling in any continuous process considered for commercial application. PE formation is complex and can be exacerbated by different variables such as reaction conditions or the catalyst structure.[14] However, it is interesting to note that low catalyst activity generally translates into higher PE content as demonstrated in Table 3 with respect to different PNP ligand motifs (Figure 8). In Table 3, only PE selectivities are shown, the rest of the total product resulted from selective ethylene oligomerisation.

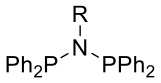

1a: R = CH_3

2: R = $CH_2CH(CH_3)_2$

3: R = $CH(CH_3)_2$

Figure 8. PNP ligand motifs.

Table 3. Relationships between catalyst activity and PE formation.[a]

Ligand	Total activity [10^6 g/gCr/h]	% PE	PE activity [10^4 g/gCr/h]
1a	0.62	3.3	2.05
2	1.14	1.0	1.14
3	1.50	0.3	0.45

[a] Conditions: 100 mL Methylcyclohexane (MCH), 2.5 µmol $Cr(acac)_3$, 1.1 equiv. ligand, 960 equiv. Al, 45 bar, 60 ˚C, ethylene fed to reactor = 160g. 1-C8 = 1-octene, 1-C6 = 1-hexene.

The results indicate that PE activity decreases with increasing oligomerisation activity. Furthermore, whether selective ethylene oligomerisation is slow or fast, PE formation is always relatively slow (more than an order of magnitude slower). This may indicate that a different, possibly neutral, Cr catalyst[36] is involved in the sluggish PE formation, particularly in view of the fact that the cationic Cr-complexes[37] are known to be involved in highly active polymerisation of ethylene. (However, the alternative possibility that low concentrations of a cationic Cr-species, different from that responsible for ethylene oligomerisation, could be responsible for the slow ethylene polymerisation cannot be excluded.)

It is therefore suggested that the competition between oligomerisation and polymerisation is related to the equilibrium between neutral and cationic catalytic Cr species. More specifically, it is suggested that neutral catalytic species give rise to (generally slow) ethylene polymerisation, while cationic catalytic species support (generally fast) selective ethylene oligomerisation. The important role of ligand steric bulk in such equilibria has been shown in a DFT-based study on the role of MAO in catalyst activation.[28] It was earlier mentioned that increased ligand steric bulk can accelerate the reductive elimination step. In addition, increased ligand steric bulk could possibly stabilize the cationic Cr species which would result in increased oligomerisation reaction rates.

Improved catalyst activity resulting from increased steric bulk and steric interactions is also demonstrated by dramatic increases in catalytic activity of diphosphine ligands with one[38] or two[39-40] carbon linkers. However, too much ligand steric bulk could impede ethylene coordination to the catalyst. The correlation between catalytic activity and PE formation is also reflected in publications involving other bidentate ligand motifs as well as with tridentate ligands.[41-42]

Conclusion

It was shown that increasing the steric bulk on the N-substituent of PNP ligands or by adding *ortho*-substituents on the phenyl rings of the PNP ligand motif resulted in a decrease in C6 cyclics and C16+ by-products with initial gains in 1-octene and 1-hexene, followed by a further increase in 1-hexene and a loss in 1-octene. This step-wise shift in selectivity can be explained mechanistically: C6 cyclics and C16+ by-products share a common intermediate, which is highly sensitive to changes in ligand steric bulk. Further increases in steric bulk suppress formation of the metallacyclononane (which leads to 1-octene) and favour formation of the metallacycloheptane (which leads to 1-hexene).

It was also observed that catalyst activity increases with increasing steric bulk (up to a maximum) and higher catalyst activity is normally associated with lower polyethylene formation. Given that increased ligand steric bulk can promote cationisation of the catalyst, it is proposed that neutral catalytic species are involved in (generally slow) ethylene polymerisation while cationic catalytic species are responsible for (generally fast) selective ethylene oligomerisation.

Previous work has primarily focused on 1-octene selectivity. This publication demonstrates that other by-products as well as catalyst activity can also be correlated to catalyst structural properties.

Experimental Section

Ligand Synthesis

Synthesis of the PNP ligands have been reported elsewhere.[15,29,43-44] The typical procedure is as follows: To a stirred solution of amine (19.6 mmol) in acetonitrile was added triethylamine (41.6 mmol). Ph_2PCl (42.9 mmol) was then added in portions. After the addition, the reaction mixture was stirred overnight at room temperature. The mixture was concentrated and the residue was slurried with diethyl ether or THF (ca. 100 mL). The $[Et_3NH]^+Cl^-$ salt was filtered by passing through a short activated alumina column. Filtration was repeated until a pure product was obtained. The solvent was evaporated to give the desired ligand.

General catalytic techniques

The sensitivity of the catalyst species towards moisture and air required all procedures to be carried out under dry, inert conditions. This was accomplished by working either in a glove box, or using standard Schlenk line techniques. All catalyst preparations were carried out in flamed-out glass Schlenk tubes. Solvents were pre-dried by percolation through neutral alumina or through an MBraun auto-percolation apparatus. $Cr(acac)_3$ and solvents were purchased from Sigma Aldrich. The methylaluminoxane was obtained from Akzo-Nobel. Ethylene 3.5 was supplied by Air Liquide or Linde AG. The Al to Cr ratio used was 960 eq. unless otherwise stated. The catalyst concentration solutions employed in reactions were 2.5 µmol Cr and 2.75 µmol ligand in 100 ml reaction solvent (methylcyclohexane).

Catalytic runs were carried out in 450 ml Parr autoclaves (unless indicated otherwise) fitted with internal cooling coils, baffles and a gas entrainment stirrer. Ethylene uptake during catalysis was monitored by Danfoss (Type Mass 6000) flowmeter. Unless indicated otherwise, all

reactions were conducted at 60 ˚C and 45 bar ethylene pressure with a total catalyst and solvent volume of 100 ml.

The HP model 6890 gas chromatograph equipped with a flame ionization detector and split injection mode was used for GC analysis. The instrument was fitted with a PONA capillary column (50m x 0.25mm id x 0.25 µm), using hydrogen as carrier gas. The temperature program used for the analysis of all ethylene oligomerisation reaction product mixtures was as follows: Initial temp: 50 °C; Initial time: 5 min.; Rate 6 °C/min; Final temp: 300 °C; Final time: 10 min.

Catalytic reaction procedure

The reactor was allowed to cool to room temperature under nitrogen following heating at 120 ˚C under vacuum for one hour. The pre-weighed reaction solvent was added to the reactor and then heated to the operating temperature. The desired ligand was dissolved in 25 ml of solvent and an aliquot combined with the chromium catalyst solution in a Schlenk vessel and stirred for ca. 5 minutes. The resulting solution/suspension was then transferred to the Parr reactor following addition of the activator. The reactor was then immediately charged with ethylene to the desired pressure and the reaction temperature was controlled by circulating water through the cooling coils during the course of the catalytic run. Ethylene was fed on demand and thorough mixing was ensured by stirring at rates of 1200 rpm or more. The reaction was terminated after 160 g of ethylene was fed to the reactor followed by cooling the reactor contents using ice to around 10 °C. Following careful releasing of the excess ethylene from the autoclave, the reaction mixture was then quenched with ethanol. Nonane was then added to the reaction mixture as a standard and the liquid phase was analysed by GC-FID. The remainder of the organic layer was filtered to isolate the polymeric material, which was dried in an oven overnight and weighed.

Computational details

All geometry optimizations were performed with the DMol^3 density functional theory (DFT) code [45-47] as implemented in the MaterialsStudio (Version 3.2) program available from Accelrys Inc. Nonlocal generalized gradient approximation (GGA) exchange correlation functionals were used in this study, i.e., the PW91 functional of Perdew and Wang.[36]

DMol^3 utilises a basis set of numeric atomic functions, which are exact solutions to the Kohn-Sham equations for the atoms.[48] These basis sets are generally more complete than a comparable set of linearly independent Gaussian functions and have been demonstrated to have small basis set superposition errors.[48] In the present study an all-electron polarised split valence basis set, termed double numeric polarised (DNP), has been used. All geometry optimisations employed highly efficient delocalised internal coordinates.[49] The use of delocalised coordinates significantly reduces the number of geometry optimisation iterations needed to optimise larger molecules compared to the use of traditional Cartesian coordinates. The tolerance for convergence of the SCF density was set to 10^{-5} hartrees, while the tolerance for energy convergence was set to $2x10^{-6}$ hartrees.

For all calculations involving chromium the SCF convergence was improved by allowing for fractional electron occupation numbers of near-vacuum energy levels by calculating a finite-temperature Fermi function. A thermal smearing of $5x10^{-3}$ hartrees was used throughout.

All calculations were performed without the incorporation of solvent effects; motivated by the fact that Cr-PNP-catalysed ethylene trimerisation/tetramerisation is commonly performed in nonpolar solvents such as toluene and cyclohexane.

Quartet (S3) spin states were calculated to be consistently lower in energy compared to the corresponding doublet (S1) spin states for all the Cr(III) complexes considered, effectively favouring a quartet (S3) ground state.

Acknowledgements

The authors thank Sasol South Africa (Pty) Ltd for funding and permission to publish this work.

Keywords: ethylene oligomerisation • ligands • reaction mechanisms • selectivity • structure-activity relationships

[1] A. Bollman, K. Blann, J.T. Dixon, F.M. Hess, E. Killian, H. Maumela, D.S. McGuinness, D.H. Morgan, A. Neveling, S. Otto, M.J. Overett, A.M.Z. Slawn, P. Wasserscheid, S. Kuhlmann, *J. Am. Chem. Soc*. **2004**, *126*, 14712-14713.

[2] M.J. Overett, K. Blann, A. Bollmann, J.T. Dixon, D. Haasbroek, E. Killian, H. Maumela, D.S. McGuinness, D.H. Morgan, *J. Am. Chem. Soc*. **2005**, *127*, 10723-10730.

[3] A.N.J. Blok, P.H.M. Budzelaar, A.W. Gal, *Organometallics* **2003**, *22*, 2564-2570.

[4] T.J.M. de Bruin, L. Magna, P. Raybaud, H. Toulhoat, *Organometallics* **2003**, *22*, 3404-3413.

[5] S. Tobisch, T. Ziegler, *Organometallics* **2003**, *22*, 5392-5405.

[6] S. Tobisch, T. Ziegler, *J. Am. Chem. Soc*. **2004**, *126*, 9059-9071.

[7] S. Tobisch, T. Ziegler, *Organometallics* **2004**, *23*, 4077-4088.

[8] S. Tobisch, T. Ziegler, *Organometallics* **2005**, *24*, 256-265.

[9] Z-X. Yu, K.N. Houk, Angew. *Chem. Int Ed*. **2003**, *42*, 808-811.

[10] W. Janse van Rensburg, C. Grove, J.P. Steynberg, K.B. Stark, J.J. Huyser, P.J. Steynberg, *Organometallics* **2004**, *23*, 1207-1222.

[11] G.J.P. Britovsek, D.S. McGuinness, R. Malinowski, J.D. Nobbs, A.K. Tomov, C.T. Young, A.W. Wadsley, *ACS Catal.* **2015**, *5*, 6922-6925.

[12] T. Agapie, S.J. Schofer, J.A. Labinger, J.E. Bercaw, *J. Am. Chem. Soc*. **2004**, *126*, 1304-1305.

[13] D.S. McGuinness, *Chem. Rev*. **2011**, *111*, 2321–2341.

[14] K.A. Alferov, G.P. Belov, Y. Meng, *Appl. Catal. A* **2017**, *542*, 71-124.

[15] K. Blann, A. Bollmann, H. de Bod, J.T. Dixon, E. Killian, P. Nongodlwana, M.C. Maumela, H. Maumela, A.E. McConnell, D.H. Morgan, M.J. Overett, M. Prétorius, S. Kuhlmann, P. Wasserscheid, *J. Catal.* **2007**, *249*, 244-249.

[16] N. Cloete, H.G. Visser, I. Engelbrecht, M.J. Overrett, W.F. Gabrielli, A. Roodt, *Inorg. Chem*. **2013**, *52*, 2268-2270.

[17] L. Falivene, R. Credendino, A. Poater, A. Petta, L. Serra, R. Oliva, V. Scarano, L. Cavallo, *Organometallics* **2016**, *35*, 2286-2293.

[18] A. Poater, B. Cosenza, A. Correa, S. Giudice, F. Ragone, V. Scarano, L. Cavallo, *Eur. J. Inorg. Chem*. **2009**, 1759-1766.

[19] A. Poater, L. Cavallo, *Dalton Trans*. **2009**, 8878-8884.

[20] S. Maley, D-H. Kwon, N. Rollins, J. Stanley, O. Sydora, S.M. Bischof, D.H. Ess, Quantum-Mechanical Transition-State Model Combined with Machine Learning Provides Catalyst Design Features for Selective Cr Olefin Oligomerization, **2020**. https://doi.org/10.26434/chemrxiv.12578552.v1.

[21] I.A. Guzei, M. Wendt, *Dalton Trans*. **2006**, 3991-3999.

[22] R.W. Taff, Steric effects in Organic Chemistry, M.S. Newman (Ed.), Wiley, New York **1956**, p 556.

[23] T. Agapie, M.W. Day, L.M. Henling, J.A. Labinger, J.E. Bercaw, *Organometallics* **2006**, *25*, 2733-2742.

[24] P. Elowe, C. McCann, P.G.Pringle, S.K. Spitzmesser, J.E. Bercaw, *Organometallics* **2006**, *25*, 5255-5260.

[25] T. Agapie, S.J. Schofer, J.A. Labinger, J.E. Bercaw, *J. Am. Chem. Soc*. **2004**, *12*6, 1304.

[26] L.E. Bowen, M.F. Haddow, A.G. Orpen, D.F. Wass, *J. Chem. Soc. Dalton Trans*. **2007**, 1160-1168.

[27] S-K. Kim, T-J. Kim, J-H. Chung, T-K. Hahn, S-S. Chae, H-S. Lee, M. Cheong, S. O. Kang, *Organometallics* **2010**, *29*, 5805-5811.

[28] W. Janse van Rensburg, J-A. van den Berg, P. Steynberg, *Organometallics* **2007**, *26*, 1000-1013.

[29] S. Kuhlmann, K. Blann, A. Bollmann, J.T. Dixon, E. Killian, M.C. Maumela, H. Maumela, D.H. Morgan, M. Prétorius, N. Taccardi, P. Wasserscheid, *J. Catal*. **2007**, *245*, 277-282.
[30] G. J. P. Britovsek, D. S. McGuinness, T. S. Wierenga, C. T. Young, *ACS Catal.* **2015**, *5*, 4152-4166.
[31] E. Naji-Rad, M. Gimferrer, N. Bahri-Laleh, M. Nekoomanesh-Haghighi, R. Jamjah, A. Poater, *Catalysts* **2018**, *8*, 224.
[32] G.J.P. Britovsek, D.S. McGuinness, *Chem. Eur. J.* **2016**, *22*, 16891-16896.
[33] J. Clayden, N. Greeves, S. Warren, P. Wothers, Organic Chemistry, Oxford University Press, New York **2001**, 1316.
[34] W-J. van Zeist, R. Visser, E.M. Bickelhaupt, *Chem. Eur. J.* **2009**, *15,* 6112-6115.
[35] M.C. Nielsen, K.J. Bonney, F. Schoenebeck, Angew. *Chem. Int. Ed*. **2014**, *53*, 5905.
[36] G. Mani, F.P. Gabbai, *Angew. Chem. Int. Ed*. **2004**, *43*, 2263-2266.
[37] B.L. Small, M.J. Carney, D.M. Holman, C.E. O'Rourke, J.A. Halfen, *Macromolecules* **2004**, *37*, 4375-4386.
[38] A. Dulai, H. de Bod, M.J. Hanton, D.M. Smith, S. Downing, S.M. Mansell, D.F. Wass, *Organometallics* **2009**, *28*, 4613-4616.
[39] M.J. Overett, K. Blann, A. Bollmann, R. de Villiers, J.T. Dixon, E. Killian, M.C. Maumela, H. Maumela, D.S. McGuinness, D.H. Morgan, A. Rucklidge, A.MZ. Slawin, *J. Mol. Catal. A Chem*. **2008**, *283*, 114-119.
[40] S-K. Kim, T-J Kim, J-H. Chung, T-K. Hahn, S-S. Chae, H-S. Lee, M. Cheong, S.O. Kang, *Organometallics* **2010**, *29*, 5805-5811.
[41] Y. Shaikh, J. Gurnham, K. Albahily, S. Gambarotta, I. Korobkov, *Organometallics* **2012**, *31*, 7427-7433.
[42] J.E. Radcliffe, A.S. Batsanov, D.M. Smith, J. A. Scott, P.W. Dyer, M.J. Hanton, *ACS Catal*. **2015**, *5*, 7095-7098.
[43] M.C. Maumela, K. Blann, H. de Bod, J.T. Dixon, W.F. Gabrielli, D.B.G. Williams, *Synthesis* **2007**, *24*, 3863-3867.
[44] J.A. Willemse, Towards selective olefin oligomerisation, PhD thesis, University of the Witwatersrand **2016**.
[45] B.J. Delley, *J. Chem. Phys*. **1992**, *92*, 508-517.
[46] B.J. Delley, *J. Chem. Phys*. **1996**, *100*, 6107-6110.
[47] B.J. Delley, *J. Chem. Phys*. **2000**, *113*, 7756-7764.
[48] B. Delley, Modern Density Functional Theory: A Tool for Chemistry; Seminario J.M., Politzer P., Eds.; Theoretical and Computational Chemistry, Elsevier, Amsterdam, Netherlands **1995**, vol. 2.
[49] J. Andzelm, R.D. King-Smith; G. Fitzgerald, *Chem. Phys. Lett.* **2001**, *335*, 321-326.

Entry for the Table of Contents

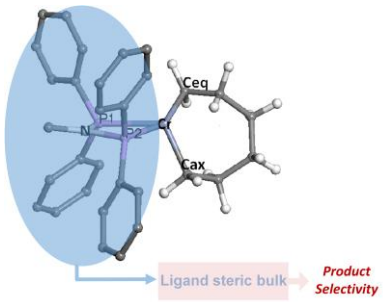

Ethylene oligomerisation is an important industrial process. The diphenylphosphinoamine (PNP) ligands are used commercially for ethylene tetramerisation. However, 1-octene selectivity rarely exceeds 70 %. In this work, PNP ligand structures are correlated with the full product selectivity. In particular, the formation of oligomeric and polymeric by-products is discussed. The correlations are supported by mechanistic interpretations.